研究成果の刊行に関する一覧表

発表者氏名	論文タイトル名	発表誌名	巻号	ページ	出版年
Iwasawa K, Tanaka G, Aoyama T, Chowdhury M M, Komori K, Tanaka-Kagawa T, Jinno H, Sakai Y	Prediction of phthalate permeation through pulmonary alveoli using a cultured A549 cell-based in vitro alveolus model and a numerical simulation.	*AATEX*	18	19-31	2013
達 晃一, 星野邦広, 岩崎貴普, 曽根孝, 何 佳, 神野透人, 加藤信介	プレート吸着によるSVOCs評価法の基礎検討：DEHPの評価方法	空気調和・衛生工学会論文集	197	19-26	2013
Zhou Z., Zhao B., Kojima H., Takeuchi S., Takagi Y., Tateishi N., Iida M., Shiozaki T., Xu P., Qi L., Ren Y., Li N., Zheng S., Zhao H., Fan S., Zhang T., Liu A., Huang Y.	Simple and rapid determination of PCDD/Fs in flue gases from various waste incinerators in China using DR-EcoScreen cells.	*Chemosphere*	102	24-30	2014
Takeuchi S., Kojima H., Saito I., Jin K., Kobayashi S., Tanaka-Kagawa T., Jinno H.	Determination of 34 plasticizers and 25 flame retardants in indoor air from houses in Sapporo, Japan.	*Sci Total Environ*	491-492	28-33	2014

IV. 研究成果の刊行物・別刷

ORIGINAL ARTICLE

Prediction of Phthalate Permeation Through Pulmonary Alveoli using a Cultured A549 Cell-based in Vitro Alveolus Model and a Numerical Simulation

Kokoro Iwasawa[1], Genya Tanaka[1], Takuya Aoyama[1], Mohammad Mahfuz Chowdhury[1], Kikuo Komori[1], Toshiko Tanaka-Kagawa[2], Hideto Jinno[2] and Yasuyuki Sakai[1]

[1]Institute of Industrial Science, The University of Tokyo, Tokyo, Japan
[2]National Institute of Health Sciences, Tokyo, Japan

Abstract
The animal-free prediction of inhalation toxicities in the lungs is very important concerning various low-volatile organic carbons such as phthalate. Phthalate are contained in plastics as plastisizer, easily released into environment as plastic ages, and ingested through dust. We therefore investigated benzylbutyl phthalate (BBP) permeation using an A549 cell-based lung alveolus model, in which the cell monolayers were formed on semipermeable membranes between two chambers filled with cell culture medium. With kinetic parameters obtained via these experiments, the model largely described the concentration changes in the three compartments (the apical, A549 cell, and basolateral layers) but revealed very high BBP accumulation in the alveolus cell layer at equilibrium, which did not likely reflect the in vivo situation. We therefore changed the parameter of thickness of the cell layer from 10 (cultured A549 cells) to 0.5 μm (alveoli) and the parameter of the concentration in basolateral compartment to be always zero because of the continuous perfusion of blood in vivo. After changing these parameters, the accumulation of BBP remarkably decreased, and the total permeated amount significantly increased. These results indicated that various parameters and assumptions should be changed to overcome the limitations and/or properties of existing culture models to improve the predictive accuracy of the system when using in vitro cell-based tissue models and numerical simulations to predict health hazards in humans.

***Key words**: in vitro, phthalate, alveolus, Numerical model*

Introduction

Various phthalic acid esters (PAEs) have been widely used as plasticizers in a variety of consumer products and household industries (Autian, 1973; Peakall, 1975). However, phthalates are not chemically bound to the plastic polymer matrix; they can be released from products, after which they can migrate into the external environment (Giam *et al.*, 1978). It is reported that PAEs influence the metabolism of hormones involved in reproductive and developmental processes in animals (Ema *et al.*, 2000; Pan *et al.*, 2006; Salazar *et al.*, 2004; Van Meeuwen *et al.*, 2007). On assessing the effects of dibutyl phthalate (DBP) and benzylbutyl phthalate (BBP) on transactivation of the estrogen receptor and breast cancer cell growth in vitro, it was found that they were estrogenic. BBP is one of the longer phthalate molecules, and its metabolites include monobutyl phthalate (MBuP) and monobenzyl phthalate (MBeP). BBP has wide application as a plasticizer in the polymer indus-

try to improve flexibility, workability, and general handling properties; approximately 80% of all phthalates are used for this purpose (IARC, 2000). Therefore, BBP is found in a variety of products, including building materials, vinyl gloves, artificial leather, and adhesives. Since it is not commonly used in plastic toys, and thus, exposure to BBP through this route is low in infants and children (European Chemicals Bureau, 2007). However, it was suggested that ingestion of dust is a significant source of BBP exposure in young children (Wormuth *et al.*, 2006), and the source of dust is most likely building materials (Bornehag *et al.*, 2005); therefore, inhalation is the primary route of exposure to BBP.

Because of the difficulties in establishing simple in vitro pulmonary exposure systems, animal models are mainly used for toxicity tests for nanoparticles, gaseous compounds, or samples. From the standpoint of animal protection, the number of animals sacrificed in animal-based experiments must be reduced, and from the viewpoint of species differences between human and animals, it is still controversial to determine the toxicity of agents in humans on the basis of results in animal studies; thus, toxicity is generally tested using cells of human origin. Several in vitro respiratory cell systems, including static culture dishes (Patel *et al.*, 1990), dishes on tilting platforms (Dumler *et al.*, 1994; Guerrero *et al.*, 1979; Nikula *et al.*, 1990), rotating flasks (Banks *et al.*, 1990; Pace *et al.*, 1969), roller bottles (Bolton *et al.*, 1982), bubbling gas through cell suspensions (Konings, 1986), and gas permeable membranes with culture medium above the cells and gas flow beneath them (Alink *et al.*, 1980; Cheek *et al.*, 1988), have been proposed. However, it is impossible to conclude whether these systems completely mimic the in vivo situation.

In this study, we established a three-compartment model to clarify the dynamics of phthalates around the alveolar epithelial cell layer and predict the permeation and accumulation of phthalate in vivo in combination with a numerical simulation method. Although it is important to determine the toxicity associated with exposure via inhalation, in vitro research on the toxicity of phthalate and its translocation in the pulmonary system using culture inserts (Shimizu *et al.*, 2004; Komori *et al.*, 2008) has not been reported. We focused on the toxicity of BBP and its metabolites MBuP and MBeP and measured the permeation of BBP through an alveolar epithelial cell layer formed on a culture insert containing a polyester membrane to divide the apical and basal compartments. The apical compartment mimics the air in alveoli, and the basal compartment mimics pulmonary intravenous blood. Even in this system, inappropriate parameters concerning the thickness of the cell layer and the concentration of the chemicals in the basal compartment were present. To mimic the in vivo situation, we therefore changed these inappropriate parameters to elucidate the dynamics of BBP in and around alveolar epithelial cell layers.

Materials and Method

Cell culture and medium

A549 cells (ATCC® CCL-185™), which is human alveolar basal epithelial cells, and HepG2 cells(ATCC® HB-8065™), which is Human hepatocellular liver carcinoma cell line were obtained from Riken Gene Bank (Tsukuba, Japan). The cells were cultured in Dulbecco's Modified Eagle's Medium (DMEM; WAKO, Japan) supplemented with 10% fetal bovine serum (FBS; HyClone Laboratories, Inc., Waltham, MA, USA), 20 mM hydroxyethylpiperazine-*N*'-2-ethanesulfonic acid (HEPES; Dojindo, Kumamoto, Japan), and 1.0% antibiotics (A.A., Invitrogen, Drive Rockville, MD, USA). The solution of 0.25% trypsin and 0.02% EDTA in phosphate-buffered saline (PBS) was used for the cell culture passaging.

Measurement of cellular carboxylesterase (CES) activity

Diester phthalate is degraded into mono phthalate and alcohol in vivo by CES, which is present in all epithelial cells. The *p*-nitrophenyl acetate assay was performed to estimate CES activity in A549 cells based on the *p*-nitrophenol concentration produced from *p*-nitrophenyl acetate by CES (Hosokawa *et al.*, 2002). The HepG2 human hepatocyte cell line has abundant endogenous CES (Ross *et al.*, 2012); therefore, CES activity was compared between A549 and

HepG2 cells. The cells were suspended in PBS in a 15-mL tube and sonicated for 15 min. After centrifugation at 7100 rpm for 30 min, the protein concentration of the supernatant was measured, and a solution containing 20 μg/mL protein was prepared. In a 96-well plate, 100 μL of the solution was added to each well and maintained for 30 min at 37°C. Then, 100 μL of 200 mM *p*-nitrophenyl acetate was added to each well of the plate, incubated for 30 min; and the resulting amount of *p*-nitrophenol produced was measured (λ = 405 nm) using a spectrophotometer (MPR-4Ai, Tosoh, Co., Japan) to determine the level of CES activity in the cells.

Cytotoxicity assay

Chemical toxicities in A549 cells were quantitatively examined using the acid phosphatase (AP) assay, which determines the number of living cells based on AP activity(Yang *et al.*, 1996; Martin *et al.*, 1993). After exposing A549 cells to phthalate for the specified times, the cells were carefully rinsed twice with PBS to remove any dying or loosely attached cells. The cells were then exposed to 0.25 M acetate buffer solution (pH 5.5) containing 10 mM *p*-nitrophenol phosphate (Wako) as a substrate for acid phosphatase and 0.01% Triton X-100 as a cytomembrane destruction reagent for 2 h at 37°C in an incubator; the resulting *p*-nitrophenolate produced was measured using an MPR-4Ai spectrophotometer (λ= 405 nm) to determine AP activity in the cells remaining on the membrane surfaces. The % viability R was determined using the following equation:

$$R = 100 \times \frac{A_S - A_0}{A_C - A_0},$$

where A_s and A_c are the absorbance values after phthalate exposure and of the medium only, respectively, and A_0 is the control absorbance value.

Formation of an A549 cell layer on a membrane culture insert

After being coated with a collagen solution containing 10% collagen (Cell matrix Type I-P, Nitta Gelatin, Osaka, Japan) and exposed to 1 mN HCl in Milli-Q water for 1 h in the refrigerator, a polyester membrane culture insert with a culture a culture surface area of 1.0 cm^2 and a pore size of 0.4 μm (Transwell 3460, Coster, Cambridge, MA, USA) was washed with culture medium, and A549 cells were seeded at a density of 5.0×10^4 cells/cm^2 onto the insert. The level of confluence of the cell sheet was determined by measuring its transepithelial electrical resistance (TEER), reflecting the function of tight junctions, using a Millicell-ERS (Millipore Corp., Bedford, MA, USA), and the time course formation of a cell layer was assessed. The TEER value gradually increased over time and reached a steady state at approximately 45 Ω·cm^2 by the 7th day. Therefore, A549 cells were cultured for 7 days in subsequent experiments.

Measurement of BBP and its two metabolites in culture medium

The phthalates examined in this study are listed in Figure 1; three major phthalates (DEHP, DBP, BBP) are widely used as plasticizers, and 3 monophthalates [mono (2-ethylhexyl) phthalate (MEHP), MBuP, and MBeP] are metabolites of the three phthalates listed in Figure 1. The standard solutions prepared for all six aforementioned phthalates and all special grade chemicals were purchased from WAKO Pure Chemical Industries, Ltd. Japan.

The A549 cells monolayer was formed on a polyester membrane as described previously. BBP was once mixed with FBS, subsequently mixed with DMEM containing FBS, HEPES, and antibiotics, to form DMEM-10% FBS-2%HEPES-1% antibiotics solution. Then, 1–10 mM BBP dissolved in culture medium was added to the culture insert (apical side; Ap) cultured with A549 cells, or 0.33–3.3 mM BBP was added to the well under the culture insert (basolateral side; BL). After 48 h, 50 μL culture medium was taken from each compartment and then mixed with 50 μL acetonitrile. To separate the supernatant from precipitated proteins and cell debris, the mixtures were centrifuged at 4000 rpm for 10 min. The concentrations of phthalate and its metabolites in the supernatants were measured by HPLC (HIC-6A, Shimazu, Japan) with a reverse-phase column (Xbridge Shield RP18, Waters, USA). The measurement conditions followed the manufacturer's recommendations. The eluent was acetonitrile:

water:formic acid (15:85:0.085 by volume) with a flow rate of 1.2 mL/min, and the excitation and emission wavelengths were 254 nm.

For the measurements of time-dependent BBP concentrations, A549 cells were seeded at a density of 5.0×10^4 cells/cm^2 onto a 10-cm tissue culture dish or culture inserts (Costar 3460, Coster, Cambridge, MA, USA) and incubated for 7 days to permit the formation of a monolayer on the bottom of the dish. The concentration of BBP in the culture medium was 10 mM for the cells cultured in the 10-cm dish, and the BBP concentration in the medium was measured by HPLC at least once per day.

Results and Discussion

CES activity of A549 cells

The *p*-nitrophenyl acetate assay was performed to estimate CES activity in A549 and HepG2 cells based on the *p*-nitrophenol concentration produced from *p*-nitrophenyl acetate by CES. The concentration of *p*-nitrophenol was measured for 5 h, and the results are shown in Fig. 2. The concentration of *p*-nitrophenol increased over time and reached saturation at approximately 3 h. Although the *p*-nitrophenol level in A549 cells was significantly lower than that in HepG2 cells, its concentration in A549 cells was considerable, indicating that CES activity in these cells is indispensable. Because CES de-

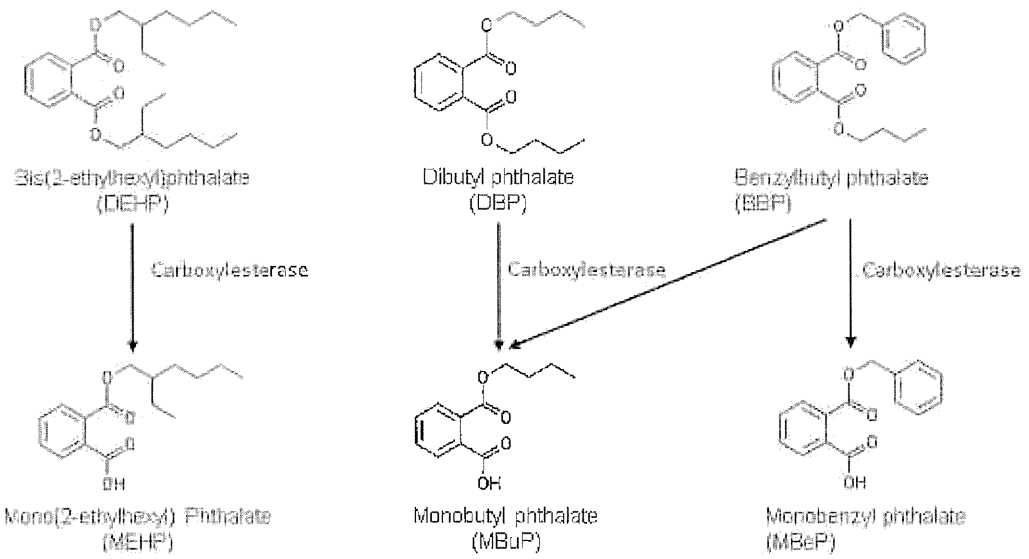

Figure 1 Phthalates examined in this study.
Three monophthalates are metabolized from the three presented phthalates.

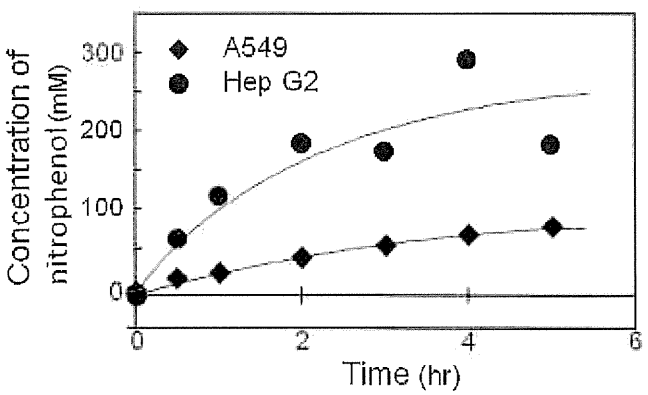

Figure 2 The concentration of p-nitrophenol metabolized from p-nitrophenyl acetate by A549 (◆) and HepG2 cells (●). Solid lines are the fitted line by least square approximation.

grades diester phthalates into monoesters, even if only a diester phthalate such as BBP was added to the cells, its monoester metabolites may exist. This result prompted us to investigate the presence of BBP and monoester phthalates such as MBuP and MBeP.

Cytotoxicity of BBP and its two metabolites MBuP and MBeP

The toxicity of BBP and its metabolites MBuP and MBeP in A549 cells at 48 h was measured by the AP assay, and the dose-response curves are presented in Fig. 3. T-test values between BBP-MBeP, BBP-MBuP and MBeP-MBuP are 0.046, 0.015 and 0.68, respectively. A549 cell viability decreased as the concentration of BBP increased. By contrast, the A549 cell viability did not decreased in the presence of MBuP and MBeP at concentrations less than 3 mM, and their viability decreased only in the presence of MBeP and MBuP at enormously high concentrations of 10 mM. It was revealed that the toxicity of BBP was higher than that of MBeP and MBuP, and both metabolites had remarkable lower toxicity than their original chemical on a molar basis. In terms of chemical structures of BBP and its two metabolites as shown in Fig. 1, BBP lacks the hydroxy group possessed by both monoesters and is considered more hydrophobic than MBuP and MBeP. In Fig. 3, the result is consistent with the principle that hydrophobic compounds are generally more toxic than hydrophilic compounds (Vesterkvist *et al.*, 2012).

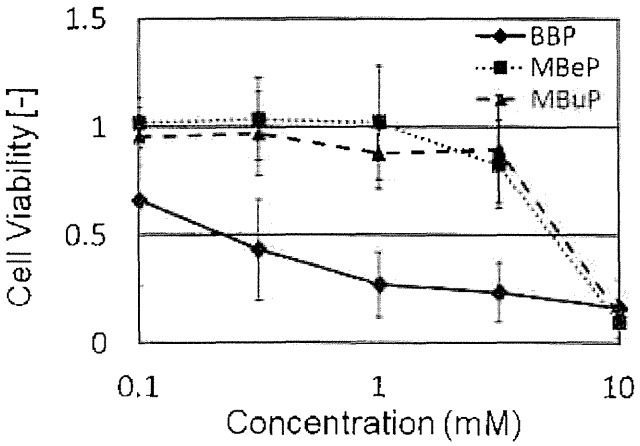

Figure 3 Dose-response curves of benzylbutyl phthalate (BBP, ◆), monobenzyl phthalate (MBeP, ■), and monobutyl phthalate (MBuP, ▲) in A549 cells 48 after phthalate was loaded into the culture medium.

Formation of two metabolites from BBP and their permeability through A549 cell layers

Medium containing BBP at one of three different concentrations (1.0, 3.2, or 10 mM) was initially added to the Ap side of the culture inserts, or medium containing 0.33, 1.1, or 3.3 mM BBP was added to the BL side. The average concentrations of BBP were 0.25, 0.79, and 2.5 mM for the three concentrations, respectively, regardless of whether BBP was added to the Ap or BL side. These average concentrations are based on the assumption that BBP is homogenously dispersed in the Ap and BL sides without the cell layers. In all cases and compartments, the concentration of MBuP was approximately 0.1 mM, which was higher than that of MBeP, indicating that MBuP was more commonly produced as a metabolite than MBeP. This finding has also been reported previously in vivo (Nativelle *et al.*, 1999).

At the same time, in all cases, the concentration of BPP was much higher than that of MBuP and MBeP in all compartments and was more than 10-fold higher in the concentration range of 1–10 mM (average, 2.5 mM). In addition, it was found that the toxicity of MBuP and MBeP was far lower than that of BBP in this study. Considering these results, we concluded that the concentrations of the BBP metabolites are negligible in the subsequent numerical simulation.

The BBP concentrations were almost identical on the Ap and BL sides 48 h after BBP was loaded on the BL side. Meanwhile, the concentration of BBP was 3~4 -fold higher on the Ap side than on the BL side when BBP was initially loaded on the Ap side. In addition, the permeability of BBP was higher when high concentrations of BBP were loaded on the Ap side. With these results, it was considered that the transport rate of BBP from the pulmonary alveoli to the blood side is minuscule (or BBP is being antiported), whereas that in the opposite direction is relatively high.

Construction of a compartment model and determination of its parameters from the permeation experiments

To summarize the above results, BBP is degraded to monophtalate MBuP and MBeP by CES, and the level of CES activity in human pulmonary epithelial A549 cells is not as high as that in human hepatocyte HepG2 cells but is not negligible (Fig. 2). Furthermore, BBP applied to A549 cells is metabolized to MBuP and MBeP, but the concentration of the metabolites are relatively low (Fig. 4). At the same time, the toxicities of these monoesters are significantly lower than that of BBP (Fig. 3); therefore, we concluded that the effect of MBuP and MBeP could be negligible for further analysis.

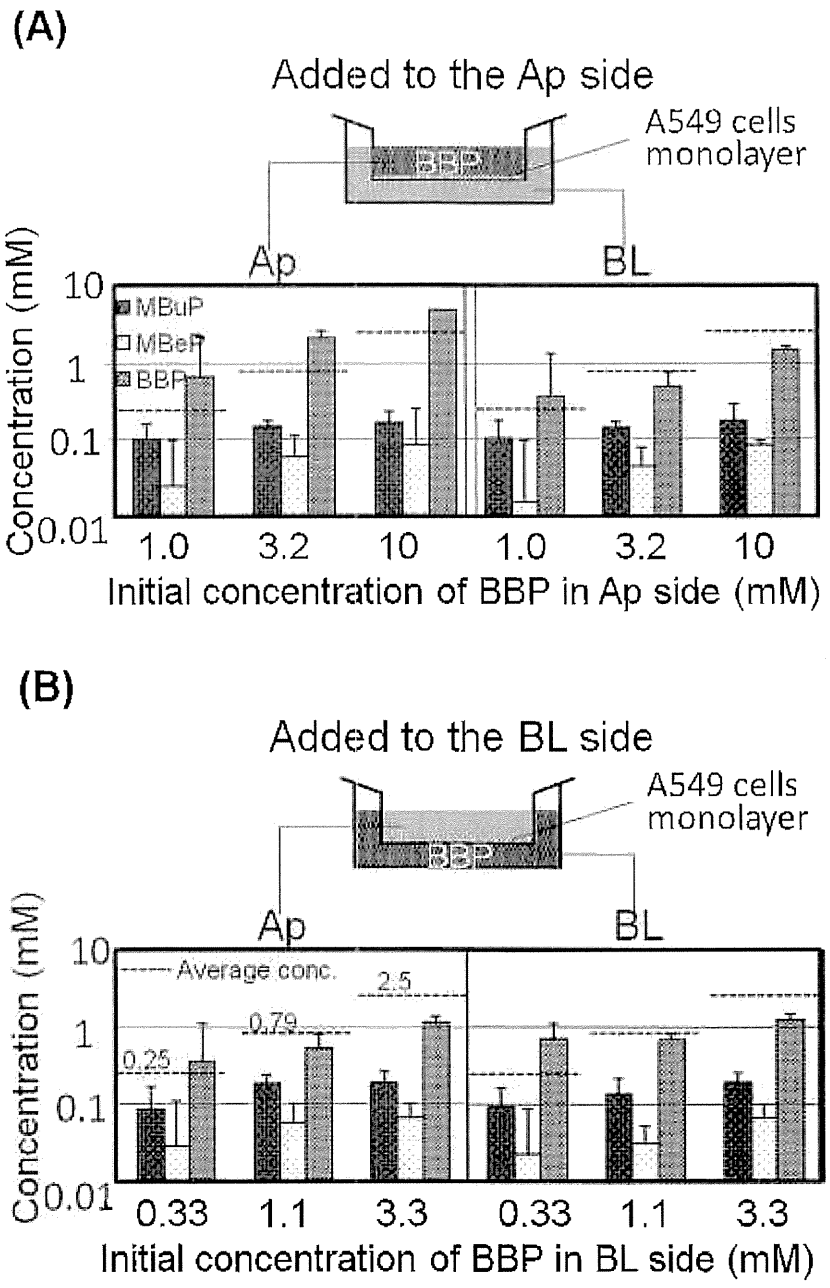

Figure 4 The amounts of monobutyl phthalate (MBuP), monobenzyl phthalate (MBeP), and benzylbutyl phthalate (BBP) on the apical (Ap) and basolateral (BL) sides 48 h after adding BBP to the Ap (A) or BL (B) side. BBP was metabolized to MBuP and MBeP, and a portion of the metabolites permeated through the cells.

Based on the aforementioned results, the following three points were considered in the analysis of long-term exposure of BBP in the mathematical model:

1 BBP is toxic to cells at concentrations exceeding 0.1 mM.
2 The effects of MBuP and MBeP are negligible.
3 The concentration of BBP on the Ap side (pulmonary alveolus side) is 3–4-fold higher than that on the BL side (blood) 48 h after loading BBP on the Ap side, whereas the BBP concentrations were nearly identical on both sides when BBP was initially added to the BL side.

Therefore, the transport of BBP from the Ap side to the BL side (from alveoli to blood) is considered very slow compared with that in the opposite direction. Conversely, BBP antiport may be occurring.

In consideration of these points, the numerical model comprising three compartments, the Ap side (inner space of the pulmonary alveolus), cell layer (alveolus epithelium), and BL side (pulmonary blood circulation) compartments, was developed by assuming dynamic equilibrium among the three compartments. BBP is transferred by the following four processes:

i. Transport from the Ap side to the cells
ii. Transport from the cells to the Ap side
iii. Transport from the cells to the BL side
iv. Transport from the BL side to the cells

Figure 5 shows these processes, compartments, and the material balances in each compartment. From the Ap side to the cell layer (i), BBP transport occurred through the lipid bilayer of the cell membrane, and the rate of transfer depended on the BBP concentration. The transfer rate is proportional to the transfer coefficient; therefore, the transportation in this process is represented by the following formula:

$$J = -k_1 \cdot \mathrm{A} \cdot C_{Ap}$$

where k_1 is the mass-transfer coefficient of (i), A is the area of transfer, and C_1 is the concentration on the Ap side. The transfer rate of BBP from the cell layer to the Ap side (ii) is proportional to the transfer coefficient. Thus, transportation in this process is represented by the following formula:

$$J = -k_2 \cdot \mathrm{A} \cdot C_{CL}$$

where k_2 is the mass-transfer coefficient of (ii) and C_{CL} is the concentration in the cell layer. Transportation in process (iii), which was the same as that in process (i), is represented by the following formula:

$$J = -k_3 \cdot \mathrm{A} \cdot C_{CL}$$

where k_3 is the mass-transfer coefficient of (iii), and transportation via this process is represented by the following formula:

$$J = -k_4 \cdot \mathrm{A} \cdot C_{BL}$$

where k_4 is the mass-transfer coefficient of (iv) and C_{BL} is the concentration on the BL side.

To determine these parameters (k_1 – k_4), and A549 cells were cultured on the membrane

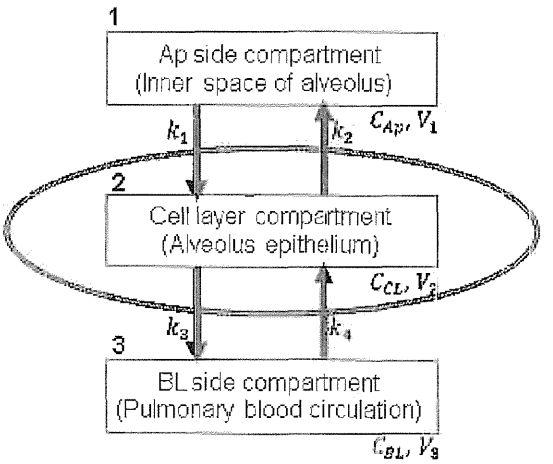

1. $V_1 \cdot dC_{Ap}/dt = (-k_1 \cdot C_{Ap} + k_2 \cdot C_{CL}) \cdot A$
2. $V_2 \cdot dC_{CL}/dt = (k_1 \cdot C_{Ap} - (k_2 + k_3) \cdot C_{CL} + k_4 \cdot C_{BL}) \cdot A$
3. $V_3 \cdot dC_{BL}/dt = (k_3 \cdot C_{CL} - k_4 \cdot C_{BL}) \cdot A$

C_i : concentration in the compartment i
V_i : volume of the compartment i
k_i : mass-transfer coefficient

Figure 5 The numerical model composed of three compartments: apical side (inner space of the alveolus), cell layer (alveolus epithelium), and basolateral side compartments (pulmonary blood circulation). BBP is transferred by four processes, and the three equations represent the material balances in each compartment.

in the culture insert and BBP-containing medium was added onto the A549 monolayer. In both experiments, the changes of the BBP concentration were measured for 48 h. The results for these experiments are shown as solid circles in Fig. 6 (a) and (b), respectively.

In the system in which monolayer cells were cultured in a tissue culture dish, there are only two compartments, the Ap side (inner space of alveolus) and cell layer compartments (alveolus epithelium), and the material transfer equations for each compartment are as follows:

$$\text{Ap side: } V_1 \cdot dC_{AP}/dt = (-k_1 \cdot C_{AP} + k_2 \cdot C_{CL}) \cdot A \quad (1)$$

$$\text{Cell layer: } V_2 \cdot dC_{CL}/dt = (-k_1 \cdot C_{AP} + k_2 \cdot C_{CL}) \cdot A \quad (2)$$

In this system, the thickness of the A549 cell layer was assumed to be 10 μm, and the cell layer volume V_{CL} is 7.9×10^{-2} cm^3 because a 10-cm dish was used for this experiment. As C_2 was almost zero soon after BBP exposure, the equation becomes

$$V_1 \cdot dC_{AP}/dt = -k_1 \cdot C_{AP} \cdot A \quad (3)$$

where A = 79 cm^2 and V_1 = 10 cm^2. As at $T_{ex} = 0$ is calculated from the slope of the curve, it is determined to be $k_1 = 2.5 \times 10^{-2}$ cm/h at the initial BBP concentration. The slope was determined by least squared approximation with 2, 3 data around $T = 0$. Conversely, when equilibrium is attained, the mass balance in each compartment is stable, and the equation becomes

$$k_1 \cdot C_{AP} - k_2 \cdot C_{CL} = 0 \quad (4)$$

k_2 is calculated as 1.6×10^{-4} cm/h using equation (4), the total mass balance, and a saturated concentration of BBP. This saturated concentration was determined by averaging the concentrations of T = 24, 46 h.

The system in which cells are cultured in

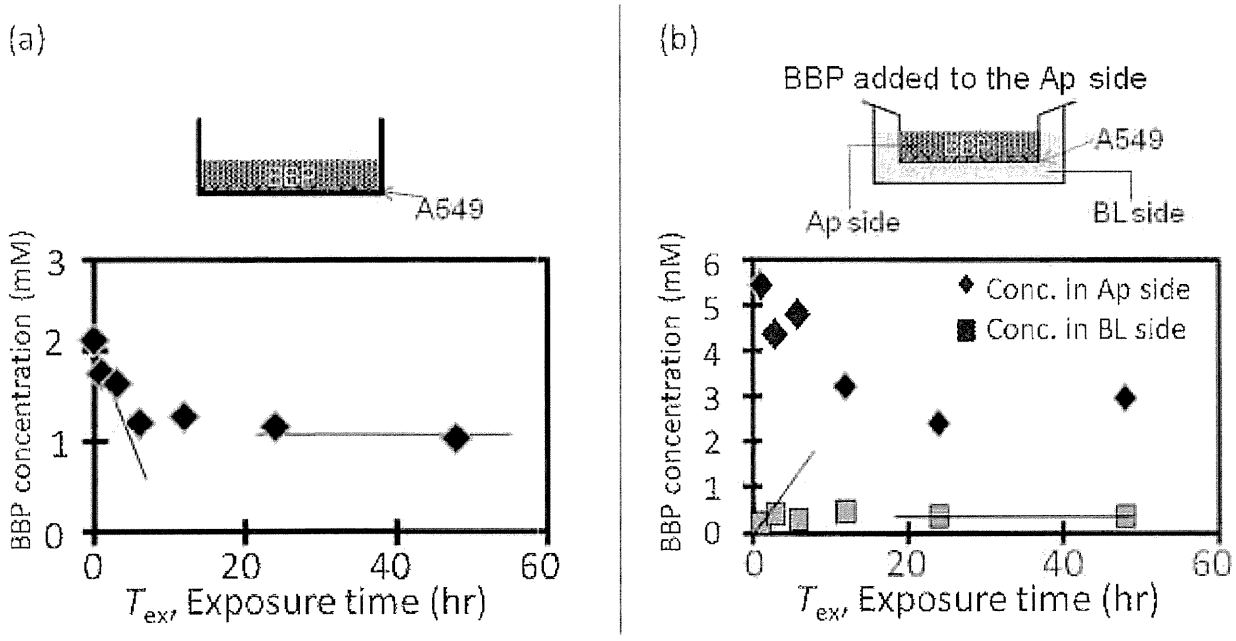

Figure 6 The time-dependent changes of the BBP concentration when cells cultured in a monolayer in a tissue culture dish (a) or on the membrane of a culture insert (b) were exposed to BBP.
The parameters (k_1-k_4) were calculated at $T_{ex} = 0$ and the equilibrium BBP concentration.

the culture insert includes all three compartments as shown in Fig. 5. The parameters (k_3 and k_4) were calculated to be 8.4×10^{-4} and 0.67 cm/h, respectively, as described previously. The calculated parameters are summarized in Table 1. With the parameters ($k_1 - k_4$) and equations (1) and (2), the time-dependent concentrations of BBP were calculated and presented as lines in Fig. 7. The calculated data were consistent with the measured data, and the correlation coefficients are 0.84 for Apical side and 0.67 for Basolateral side. It was found that the values of k_1 and k_4 were substantially higher than those of k_2 and k_3 because 10 μmol BBP at the measured value was predicted to be transported and exist in the cells in a small volume of 7.8×10^{-2} cm^3 and the BBP concentration inside the cells is extremely high; and this high concentration causes the low coefficient value of k_2 and k_3.

Prediction of in vivo BBP permeation using the simulation

The in vivo level of BBP exposure was mimicked in this study, although there were two differences between our system and the actual in vivo situation. (1) The total surface area of alveoli was reported to be 30–50 m^2, which was 4.0 $\times$ 10^5-fold greater than that in the present experiment. In addition, the thickness of alveoli was 0.5 μm compared with a thickness of approximately 10 μm in the present study (Kierszenbaum, 2007). (2) The BL side was as-

Table 1 The calculated values of parameters (k_1-k_4) with the time-dependent changes of the BBP concentration when the cells were exposed to BBP.

Parameter		
k_1	Mass transfer coefficient from Ap side to cells	2.5×10^{-2}
k_2	Mass transfer coefficient from cells to Ap side	1.6×10^{-4}
k_3	Mass transfer coefficient from cells to BL side	8.4×10^{-4}
k_4	Mass transfer coefficient from BL side to cells	6.7×10^{-1}

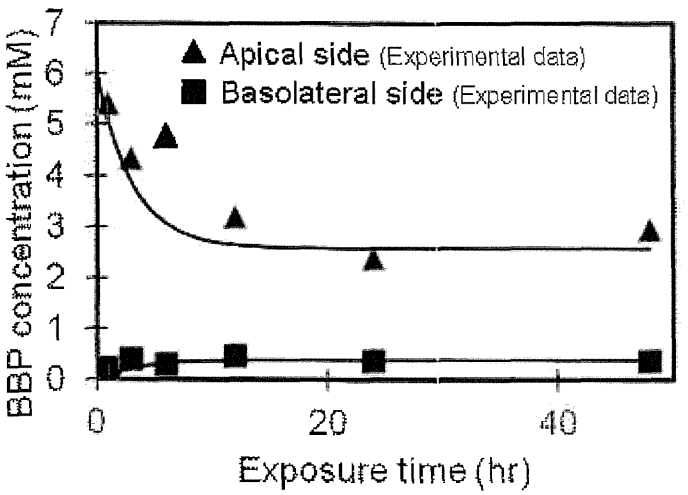

Figure 7 The time-dependent concentrations of BBP calculated using parameters (k_1-k_4) and equations (1) and (2) (shown as lines).
The calculated data are consistent with the measured data.

sumed to represent the blood, but blood is constantly perfused in the actual in vivo environment. Moreover, the perfusion rate is high, and the concentration of phthalate in blood is assumed to be zero (Ramsey *et al.*, 1984). We therefore changed the parameters concerning these points to improve the correspondence of the model to the in vivo situation.

The time-dependent amount of BBP accumulated in epithelial cells when 6,μM BBP was initially added to the cells is indicated in Fig. 8 (a), and the total amount of BBP that permeated through the cells is shown in Fig. 8 (b). The total amount of BBP in epithelial cells increased for 15 h and equilibrated at 0.30 μmol/cm^2, and the total amount of BBP permeated into the blood reached 0.13 μmol/cm^2.

First, we changed the thickness of the alveolus epithelial cell layer from 10 to 0.5 μm and calculated the total amounts of accumulated and permeated BBP as shown in the second column of Fig. 8. The total amount of accumulated BBP in cells drastically decreased compared with that at a cell thickness of 10 μm; conversely, the total amount of BBP that permeated through the cells was 0.24 μmol/cm^2, which was higher than that observed with a cell thickness of 10 μm.

In addition to changing the thickness of the cell layer, we assumed that the concentration on the BL side (i.e., the concentration of blood) was set at zero, and the calculated graphs are shown in the third column of Fig. 8. Under this condition, the BBP accumulation curve is different from the other two curves. The total amount of BBP accumulated drastically changed to 6.9 × 10^{-3} μmol/cm^2 and then gradually decreased to zero over approximately 24 h, and the total amount of BBP that permeated through the cells was 0.76 μmol/cm^2.

The simulation revealed that even if the in vitro cell-based tissue model does not perfectly

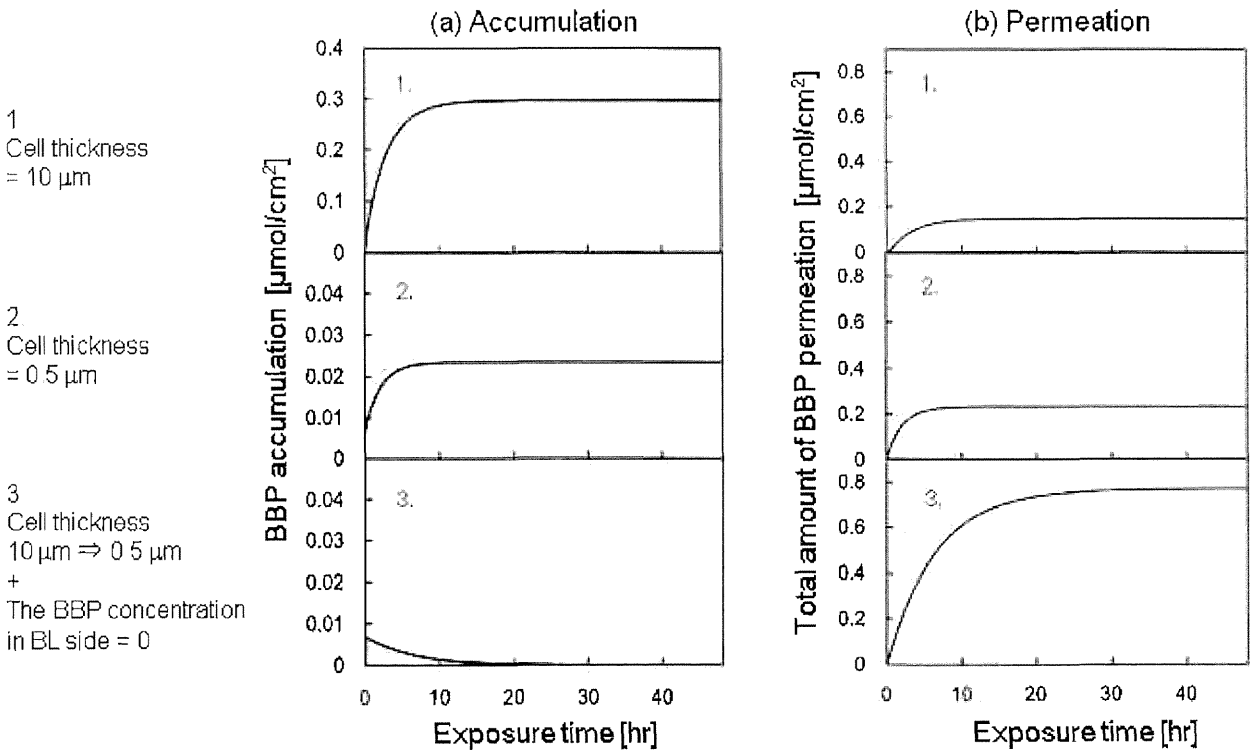

Figure 8 The time-dependent accumulation of BBP by epithelial cells (a) and the total amount of BBP permeated through the cells (b) when 6.1μM BBP was added to the apical (Ap) side.
The time-dependent curve calculated after changing the thickness of the cell layer from 10 (A549 cells) to 0.5μm (alveoli) is shown in the second column, and that when the basolateral concentration was assumed to always be zero is shown in the third column.

mimic the in vivo situation with regard to some parameters, we could overcome the limitations and/or properties of the culture models by using numerical simulations to change various parameters and assumptions in a scientifically rational manner. To predict hazards in a better manner in humans, it is important to establish an animal-free cell based model with an understanding of the parameters that differ from the in vivo condition and adjust them as needed in the numerical simulation.

From the results of the simulations, it was found that BBP inhaled into the alveoli is transported to the blood through the pulmonary epithelium for approximately 24 h in vivo as opposed to remaining in the cells. The accumulation of BBP by cells can cause epithelial damage, but the amount of BBP accumulated by cells is always less than 6.9×10^{-3} μmol/cm^2 and decreases to zero within 24 h. Therefore, these results suggest that the possibility of epithelial damage in vivo is low after BBP inhalation and these experiments using A549 cell monolayers in culture dishes could overestimate the possibility of cellular damage.

BBP, which permeates through cells to the blood, reaches other organs via the bloodstream. Previous in vivo experiments revealed that phthalate targets germ cells in the testis (David *et al.*, 2000; Lamb *et al.*, 1987). These data are consistent with the results of this study that BBP passes through cells to the bloodstream, could not be metabolized or eliminated by organs such as the liver and kidneys, and is ultimately expected to be transported to these organs (Jian, 2012). This study demonstrated that estimating the perfusion of target chemicals in the blood flow is important.

One point that should be mentioned is that the adsorption of BBP to plastics is not considered in our model. Phthalates have relatively high affinity for the surfaces of experimental instruments such as dishes and flasks, especially those made of plastic (Thomsen *et al.*, 2001). In the experiments in this study, we noticed that small amounts of BBP were lost during the procedures. These small amounts were disregarded in this study, which may result in overestimation of the amount of BBP transported to the cells. However, investigating the adsorption of BBP could be a single comprehensive subject of research because many types of plastics are used as culture apparatus and the adsorption of BBP is different for each type. In addition, adsorption is affected by conditions such as temperature, pressure, time, and the dispersion medium. Therefore, we would like to investigate this subject in a future project.

Conclusion

We identified problems in the integrated uses of permeation data for BBP in an A549 cell-based culture model using a culture insert and created a simple numerical simulation to determine the toxicity of substances in humans. The model described high accumulation of BBP in the alveolus cell layer (0.30 μmol/cm^2) at equilibrium, and therefore, we changed the thickness of the cell layer from 10 (A549 cells) to 0.5 μm (alveoli) and also incorporated the assumption that the BL concentration is always zero because the perfusion of blood in vivo. Further, the amount of accumulated BBP decreased over approximately 24 h, and the maximum amount of accumulated BBP was 6.9×10^{-3} μmol/cm^2. Moreover, the total amount of permeated BBP increased from 0.13 to 0.76 μmol/cm^2 after adjusting the aforementioned parameters. These results indicate that when in vitro cell-based tissue models and numerical simulations are used to predict toxicity in humans in an animal-free environment, various parameters and assumptions should be changed in a scientifically rational manner to overcome the limitations and/or properties of existing culture models to improve the predictive accuracy of the system.

References

Alink, G. M., de Boer, R. M., Mol, J., and Temmink, J. H. (1980) Toxic effects of ozone on human cells in vitro, exposed by gas diffusion through teflon film, Toxicology, **17**, 209–218.

Autian, J. (1973) Toxicity and health threats of phthalate esters: review of the literature, Environ Health Perspect, **4**, 3–26.

Banks, M. A., Porter, D. W., Martin, W. G., and Castranova, V. (1990) Effects of in vitro ozone exposure on peroxidative damage, membrane leakage, and taurine content of rat alveolar macrophages, Toxicol Appl Pharmacol, **105**, 55–65.

Bolton, D. C., Tarkington, B. K., Zee, Y. C., and Osebold, J. W. (1982) An in vitro system for studying the effects of ozone on mammalian cell cultures and viruses, Environ Res, **27**, 466–475.

Bornehag, C.-G., Lundgren, B., Weschler, C. J., Sigsgaard, T., Hagerhed-Engman, L., and Sundell, J. (2005) Phthalates in indoor dust and their association with building characteristics, Environ Health Perspect, 113, 1399–1404.

Cheek, J. M., Postlethwait, E. M., and Crandall, E. D. (1988) Effects of culture conditions on susceptibility of alveolar epithelial cell monolayers to NO2, Toxicol Lett, **40**, 247–255.

David, R., Moore, M., Finney, D., and Guest, D. (2000) Chronic toxicity of di(2-ethylhexyl)phthalate in rats, Toxicol Sci, **55**, 433–443.

Dumler, K., Hanley, Q. S., Baker, C., Luchtel, D. L., Altman, L. C., and Koenig, J. Q. (1994) The effects of ozone exposure on lactate dehydrogenase release from human and primate respiratory epithelial cells, Toxicol lett, **70**, 203–209.

Ema, M., Miyawaki, E., and Kawashima, K. (2000) Effects of dibutyl phthalate on reproductive function in pregnant and pseudopregnant rats. Reproductive toxicology (Elmsford, N.Y.), 14, 13–19.

European Chemicals Bureau (2007) Benzyl butyl phthalate (BBP) European Union risk assessment report. http://ecb.jrc.it/DOCUMENTS/ Existing-Chemicals/RISK_ASSESSMENT/ REPORT/ benzylbutylphthalatereport 318.pdf.

Giam, C. S., Chan, H. S., Neff, G. S., and Atlas, E. L. (1978) Phthalate ester plasticizers: a new class of marine pollutant. Science (New York, N.Y.), 199, 419–421.

Guerrero, R. R., Rounds, D. E., Booher, J., Olson, R. S., and Hackney, J. D. (1979) Ozone sensitivity in aging WI-38 cells based on acid phosphatase content, Arch Environ Health, **34**, 407–412.

Hosokawa, M. and Satoh, T. (2002) Measurement of carboxylesterase (CES) activities. Current protocols in toxicology / editorial board, Mahin D. Maines (editor-in-chief) ... [et al.], Chapter 4, Unit4.7.

IARC (2000) monographs on the evaluation of carcinogenic risks to humans. some industrial chemicals - Google 検索. International Agency for Research on Cancer, Lyon, France, pp.77.

Jian Ge (2012) Study on metabolism of N-Butyl Benzyl Phthalate (BBP) and Dibutyl Phthalate (DBP) in Ctenopharyngodon idellus by GC and LC-MS/MS. African Journal of Agricultural Research, 7(12), [online] http://www. academicjournals.org/ajar/abstracts/abstracts/abstract 2012/ 26%20Mar/ Ge%20%20et%20al.htm (Accessed December 18, 2012).

Kierszenbaum, A. (2007) Histology and Cell Biology: An Introduction to Pathology. Second Edition. Mosby . Elsevier Health Sciences, 388.

Konings, A. W. (1986) Mechanisms of ozone toxicity in cultured cells. I. Reduced clonogenic ability of polyunsaturated fatty acid-supplemented fibroblasts. Effect of vitamin E. J Toxicol Environ Health, **18**, 491–497.

Lamb, J. C., 4th, Chapin, R. E., Teague, J., Lawton, A. D., and Reel, J. R. (1987) Reproductive effects of four phthalic acid esters in the mouse, Toxicol Appl Pharmacol. **88**, 255–269.

Martin, A. and Clynes, M. (1993) Comparison of 5 microplate colorimetric assays for in vitro cytotoxicity testing and cell proliferation assays, Cytotechnol, **11**, 49–58.

Van Meeuwen, J. A., Ter Burg, W., Piersma, A. H., van den Berg, M., and Sanderson, J. T. (2007) Mixture effects of estrogenic compounds on proliferation and pS2 expression of MCF-7 human breast cancer cells, Food Chem Toxicol, **45**, 2319-2330.

Nativelle, C., Picard, K., Valentin, I., Lhuguenot, J. C., and Chagnon, M. C. (1999) Metabolism of n-butyl benzyl phthalate in the female Wistar rat. Identification of new metabolites, Food Chem Toxicol, **37**, 905–917.

Nikula, K. J. and Wilson, D. W. (1990) Response of rat tracheal epithelium to ozone and oxygen exposure in vitro, Fundam Appl Toxicol, **15**, 121-131.

Pace, D. M., Landolt, P. A., and Aftonomos, B. T. (1969) Effects of ozone on cells in vitro, Arch Environ Health, **18**, 165–170.

Pan, G., Hanaoka, T., Yoshimura, M., Zhang, S., Wang, P., Tsukino, H., Inoue, K., Nakazawa, H., Tsugane, S., and Takahashi, K. (2006) Decreased serum free testosterone in workers exposed to high levels of di-n-butyl phthalate (DBP) and di-2-ethylhexyl phthalate (DEHP): a cross-sectional study in China, Environ Health Perspect, **114**, 1643–1648.

Patel, J. M., Sekharam, K. M., and Block, E. R. (1990) Oxidant injury increases cell surface receptor binding of angiotensin II to pulmonary artery endothelial cells, J Biochem Toxicol, **5**, 253–258.

Peakall, D. B. (1975) Phthalate esters: Occurrence and biological effects, Residue Rev, **54**, 1–41.

Ramsey, J. C. and Andersen, M. E. (1984) A physiologically based description of the inhalation pharmacokinetics of styrene in rats and humans, Toxicol Appl Pharmacol, 73, 159-175.

A physiologically based description of the inhalation pharmacokinetics of styrene in rats and humans, Toxicol Appl Pharmacol, **73**, 159–175.

Ross, M. K., Borazjani, A., Wang, R., Crow, J. A., and Xie, S. (2012) Examination of the carboxylesterase phenotype in human liver, Arch Biochem Biophys, **522**, 44–56.

Salazar, V., Castillo, C., Ariznavarreta, C., Campón, R., and Tresguerres, J. A. F. (2004) Effect of oral intake of dibutyl phthalate on reproductive parameters of Long Evans rats and pre-pubertal development of their offspring, Toxicol, **205**, 131–137.

Thomsen, M., Carlsen, L., and Hvidt, S. (2001) Solubilities and surface activities of phthalates investigated by surface tension measurements, Environ Toxicol Chem, **20**, 127–132.

Vesterkvist, P. S. M., Misiorek, J. O., Spoof, L. E. M., Toivola, D. M., and Meriluoto, J. A. O. (2012) Comparative cellular toxicity of hydrophilic and hydrophobic microcystins on caco-2 cells, Toxins, **4**, 1008–1023.

Wormuth, M., Scheringer, M., Vollenweider, M., and Hungerbühler, K. (2006) What are the sources of exposure to eight frequently used phthalic acid esters in Europeans? , Risk Anal, **26**, 803–824.

Yang, T. T., Sinai, P., and Kain, S. R. (1996) An acid phosphatase assay for quantifying the growth of adherent and nonadherent cells, Anal Biochem, **241**, 103–108.

(Received: April 23, 2013/
Accepted: September 24,2013)

Corresponding author:
Kokoro IWASAWA, Ph., D.
Institute of Industrial Science,
the University of Tokyo
Department of Materials and
Environmental Science
Sakai Lab.
4-6-1 Komaba, Meguro-ku, Tokyo,
153-8505 JAPAN
Tel: +81-3-5452-6349
Fax: +81-3-5452-6353
E-mail: kokoro@iis.u-tokyo.ac.jp

空気調和・衛生工学会論文集
No. 197, 2013年8月

プレート吸着によるSVOCs評価法の基礎検討
—DHEPの評価方法—

達　晃一[*1]　星野　邦広[*2]　岩崎　貴普[*3]
曽根　孝[*4]　何　佳[*5]　神野　透人[*6]
加藤　信介[*5]

車室内VOCの低減対策のために，日本自動車工業会は車室内VOC濃度の自主規制に取り組んでいる。自主規制対象成分の中にはフタル酸エステル類などの高沸点成分が含まれているが，これら高沸点成分は従来のTenaxによる捕集では精度良く測定することが困難である。そこで，我々は高沸点成分の定量的な評価手法としてガラスプレートを高沸点成分の吸着媒体とする評価手法を検討した。本論文では高沸点成分の定量的評価手法のためのプレートの選定方法および保管方法の結果を報告する。

キーワード：解析・実験・実測・SVOCs

はじめに

車室内環境の向上を目的として，日本自動車工業会（以下JAMAと呼ぶ）は，「車室内VOC低減の自主取り組み」を公表した[1]。JAMA発表の内容によると，新型の乗用車は2007年から,新型のトラックおよびバスは2008年から厚生労働省の指針値[2]を車室内において満足させるというものである。この厚生労働省の指針値の対象成分としてフタル酸ジ-n-ブチル（以降DBPと呼ぶ），フタル酸ジ-2-エチルヘキシル（以降DEHPと呼ぶ）などの準揮発性有機化合物（以降，SVOCsと呼ぶこととした。）も含まれている。これら準揮発性有機化合物は，国土交通省所管の財団法人住宅・建築省エネルギー機構（現 建築環境・省エネルギー機構）の健康住宅研究会はSVOCsに分類される木材保存剤，可塑剤，防蟻剤の3種の薬剤を優先取り組み物質として報告[3]しており，車室内環境の向上を目的とする上では，重要な成分である。

自動車業界では2006年に自動車メーカーおよび部品材料メーカーを主体とする分科会が発足し，翌2007年1月に自動車技術会規格JASO M902「自動車部品-内装材-揮発性有機化合物（VOC）放散測定法」[4]として規格化された。しかしながら本規格で示されている測定法では，SVOCsの回収が十分ではないため過小評価[5]となる危険性がある。

一般的にSVOCsは沸点が高いため，材料から気中に放散しても，その殆どがチャンバおよびバッグの内表面や室内壁面などに吸着している。フタル酸エステルは経皮暴露も無視できないことから，表面（壁面）吸着量の測定も重要となり，気中濃度だけを測定する方法では過小評価となる危険性がある。我々の研究においてもTenaxで捕集した場合と比較して同様の結果[6]が得られている。SVOCsの沸点は高く，放散しても空気中に留まる割合が非常に少ないため，Tenaxによる空気捕集の定量結果からは，殆ど検出されていない。

Tenaxによる空気捕集法以外の評価手法として日本空気清浄協会（JACA）では，SVOCsの測定方法指針として基板表面吸着法[7]，基板表面曝露法[8]が紹介されており，ドイツの研究グループではフォギング法[9]を用いたSVOCs評価法の報告[10]がされている。これらの測定方法は，従来のTenax TAなどによる気中濃度の測定とは異なり，プレートなどに付着・吸着したSVOCsを定量評価する方法となっている。しかし，プレートの表面性状などの違いにより，吸着効率が異なるため測定結果にばらつきが発生すると推

*1 (株)いすゞ中央研究所車両研究第一部　正会員
*2 日本電子(株)　中国/アジア営業戦略室
*3 ジーエルサイエンス(株)総合技術本部CSセンターGC課
*4 エスペック(株)植物工場事業部　正会員
*5 東京大学生産技術研究所人間・社会系　正会員
*6 国立医薬品食品衛生研究所環境衛生化学部　正会員

察される。そこで，我々は，プレートの材料および表面処理の違いによる SVOCs の吸着・脱離性能評価手法の基礎検討を実施した。脱離性能については，標準試薬を用いて一般的な手法で評価を行った[11]。一方，吸着性能は実際の材料から放散した SVOCs を用いなければ評価することが困難である。そこで，本論文では，材料から放散する DEHP を利用してプレートの吸着性能の評価手法と捕集後のプレート保管方法について検討を行なったので報告する。

1. 実験手法

1.1 プレート素材の検討（材料のSVOCs放散量測定）

プレートへの SVOCs 吸着量を評価するためには，材料から継続的に安定した SVOCs の放散が必要不可欠となる。そこで，自動車部品の中から DEHP を放散する材料を選定した。今回試験に用いた材料は，PVC 製のフロアーマットである。図 - 1 にフロアーマットの外見を示す。

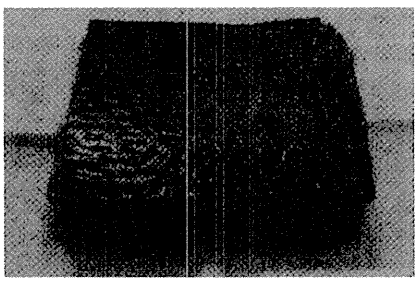

図 - 1 フロアーマット

発生ガス濃縮導入装置（以降マイクロチャンバと呼ぶ）を用いてフロアーマットからの DEHP 放散量を 9 回測定した。DEHP の分析は Tenax TA に試料ガスを捕集した後，GC/MS により定量評価を行なった。捕集および分析条件を表 - 1 に示す。部品から放散する DEHP 放散量の測定は，恒温恒湿槽を用いて，フロアーマット 5cm×5cm を 25±1℃，40±5%RH，暗所条件でアルミ箔に包んで 24 時間養生した後，マイクロチャンバで 65℃，1 時間加熱し，発生ガスを Tenax TA に捕集した。その後，部品をチャンバから取り除き，チャンバに吸着した DEHP 量を測定した。この時の温度条件は，常温から 250℃まで昇温させて，250℃で 29 分間温度を保持した。チャンバの加熱時間はトータルで約 40 分となる条件とした。チャンバ外見を図 - 2 示す。

更に，同一の部品を用いて，DEHP 放散量を約 1 年間継続して測定した。測定タイミングは月 1 回程度とし，保管は恒温恒湿槽を用いて，25±1℃，40±5%RH，暗所条件でアルミ箔に包んで保管した後，マイクロチャンバで 65℃，1 時間加熱し，発生ガスを Tenax TA に捕集した。その後，部品をチャンバから取り除き，チャンバに吸着した DEHP 量を測定した。この時の温度条件は，前述した条件と同一で，常温から 250℃まで昇温させて，250℃で 29 分間温度を保持した。チャンバの加熱時間はトータルで約 40 分となる条件とした。

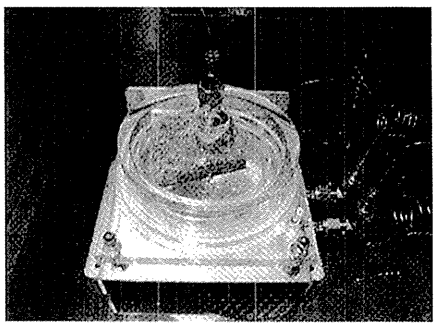

図 - 2 発生ガス濃縮装置とチャンバ

表 - 1 材料から発生する成分分析条件

発生ガス濃縮導入装置 GL サイエンス MSTD258M-B	
チャンバ	：石英 内寸φ104×H30 (内容積：254.7ml ($2.5x10^{-4}m^3$)，面積：$0.02m^2$)
パージガス流量	：捕集時 100ml/min（サイド 80ml/min、センター20ml/min），通常時 50ml/min（サイド 30ml/min センター 20ml/min）
捕集流量	：50ml/min
Pre.Purge	：0.1min（STD），3min（プレート）
ﾄﾗﾝｽﾌｧｰﾗｲﾝ温度	：270℃
オーブン温度	：常温→65℃（60min）[発生ガス] 30℃→11min →250℃（hold29min）[吸着ガス]
捕集量	：2.0L($2.0\times10^{-3}m^3$)
加熱脱着装置 Gerstel TDS	
Tube Purge	：1.0min
Desorb Temp.	：270℃
Desorb Time.	：10min
Desorb Flow	：10ml/min
Split Vent Flow	：100ml/min
Split	：1/10
He	：1mL/min
CRYO FOCUS	：Cryo -150℃, Cryo Heat temp. 270℃
GC/MS Agilent5975C	
Interface Temp.	：280℃
Ion source Temp.	：200℃
イオン化電圧	：70 eV
EM	： 0.8kV
SCAN	：35～450amu
Solvent Delay	：3min
カラム	：InertCap-5MS/Sil 0.25mm×30m *df*=0.25um， 40℃(5min)-280℃ (8min)，10℃/min

1.2 部品とプレートの配置の検討

マイクロチャンバ内に DEHP の発生源である部品（フロ

アーマット）とガラスプレート（石英ガラス製 φ80mm×2mm）をどのような配置にすれば効率の良い DEHP の捕捉が可能となるのか検討を行なった。部品の上にプレートを配置（CASE1）した場合を図 - 4 に示す。*A*：1mm, *B*：30mm と *A*：2mm, *B*：29mm で検討を行なった。図 - 3 で示したマット下に配置した丸状の治具は石英で製作したチューブ管で，マットが直接チャンバに接触することを防ぐことを目的で配置した。

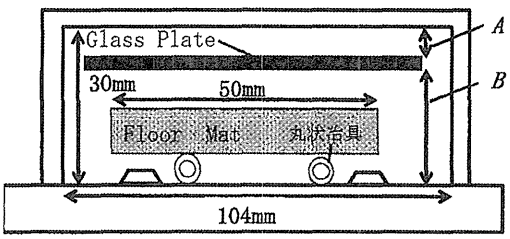

図 - 3 フロアーマットおよびプレート配置 CASE1

次に部品の下にプレートを配置（CASE2）した場合を図 - 4 に示す。*A*：5mm, 10mm で検討を行なった。CASE1, 2 いずれもフロアーマットをチャンバに設置して 65℃で発生ガスの捕集を 1 時間行なった後，フロアーマット，ガラスプレートを取り除いて，治具とチャンバに吸着したガスの測定を行なった後，プレートをチャンバに設置して，プレート単体に吸着した吸着ガスの測定を行なった。

この時の温度条件は，常温から 250℃まで昇温させて，250℃で 29 分間温度を保持した。チャンバの加熱時間はトータルで約 40 分となる条件とした。

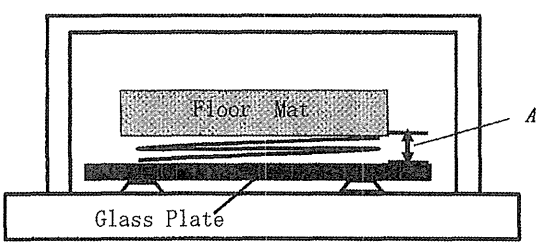

図 - 4 フロアーマットおよびプレート配置 CASE2

フロアーマットとガラスプレートを接触させた場合を CASE3, 4 として図 - 5, 6 に示す。また表 - 2 には，試験条件を示す。CASE3, 4 の温度、加熱温度および加熱時間等の測定条件は CASE1, 2 と同様である。プレートの洗浄は，メタノールおよびアセトンで表面を拭き取りその後，250℃，30 分の加熱処理をおこなった。チャンバの洗浄は 250℃，30 分の加熱処理のみとした。

表 - 2 部品とプレートとの配置の試験条件

CASE	*A* の距離 [mm]
1-1	1
1-2	2
2-1	5
2-2	10
3	-
4	-

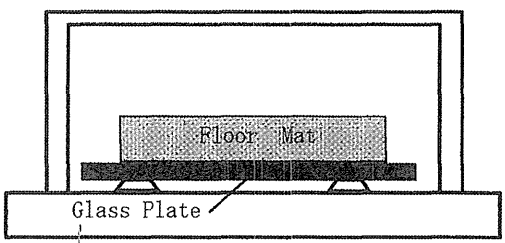

図 - 5 フロアーマットおよびプレート配置 CASE3

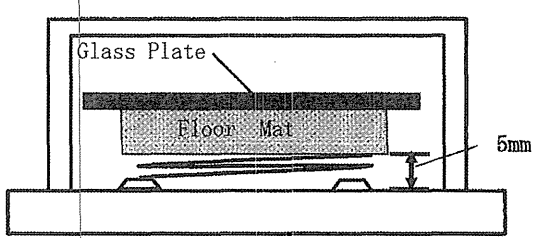

図 - 6 フロアーマットおよびプレート配置 CASE4

1.3 数値解析によるプレートへのDEHP捕捉効率の検討

1.2 で部品から揮発する DEHP を効率良く捕捉するための部品とプレートの最適配置を検討した。この最適配置の根拠となる実験的検証が困難であるため数値解析による検証を試みた。解析の境界条件を表 - 3 に，数値解析モデルを表 4 に，今回使用したチャンバ等の図面を図 - 7 に示す。

表 - 3 数値解析の境界条件

Inlet1(bottom)	流量：20ml/min=3.33×10^{-7} m^3/s 面積： 5.00×10^{-6} m^2 流 速： 0.06791 m/s *k*=0.0000166 ε=0.0000002 (*L*=0.03m)
Inlet2(side)	Zero pressure
outlet	流量：50ml/min=8.33×10^{-7} m^3/s 面積：1.26×10^{-5} m^2 流 速： 0.06631 m/s *k*=0.0000164 ε=0.00000019 (*L*=0.03m)
フロアマット表面	DEHP の表面放散速度： 1 .00×10^{-5} kg/(m^2・s)
チャンバ壁	DEHP の吸着量：吸着あり

表 - 4　数値解析の計算モデル

乱流モデル	低 Re　k-ε モデル　定常解析
差分スキーム	速度：MARS　k, ε: UD スカラー量：UD

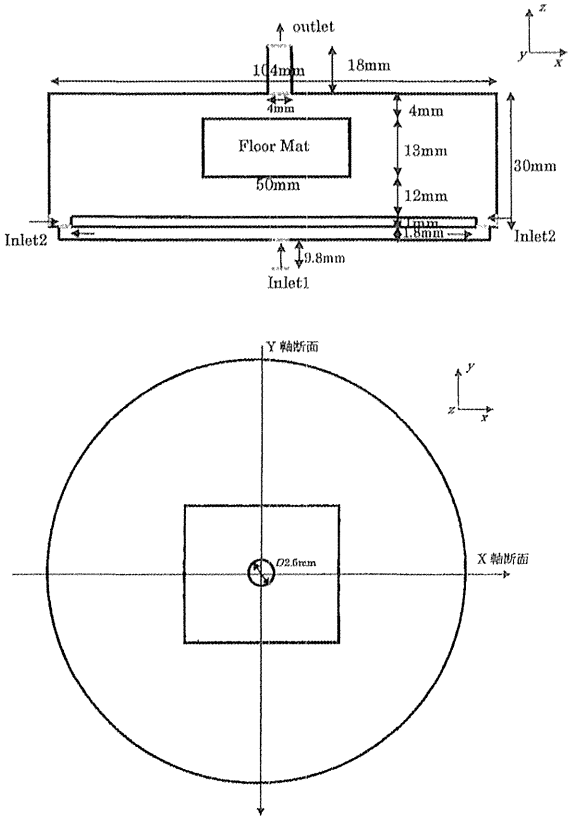

図 - 7　数値解析に用いたマイクロチャンバ図面

1.4　各種プレートのDEHP吸着量評価

1.2CASE2-2 で検討したプレートへの DEHP 吸着量評価手法を用いて，各種プレートの吸着量評価を行なった。プレートに吸着した DEHP の測定条件は，1.2 と同一である。評価したプレートの仕様を表 - 5 に示す。いずれも直径 80mm×厚み 2mm である。シリコンウエハーは厚み 0.71mm である。試験条件は表 - 1 と同一である。表 - 5 中にシリコンウエハーを選定しているが，クリーンルーム中にはクリーンルーム構成材料から発生する凝縮有機物質が存在しており，シリコンウエハー表面にこれらシロキサンやフタル酸エステル類が吸着することにより，製品性能上の不具合を引き起こすためこれらの吸着メカニズム等が研究されている[12,13]。そこで上記研究事例との比較も可能となることからシリコンウエハーを選定した。各プレートの表面性状を比較する上で，表面粗さは JIS B 0601，水接触角は JIS R 3257 に準拠して実測した値を記載した。

表 - 5　プレートの種類

名　称	仕　様	十点平均粗さ	接触角 [度]
ガラス プレート	パイレックス ガラス	0.049	84
シラン処理 プレート	ガラスプレートをジメチルジクロロシラン-トルエン溶液に浸漬させた後，乾燥	0.049	93
シリコン ウエハー	シリコン製の半導体基板	0.051	31
石英 プレート	石英製	0.050	60

1.5　SUS保管容器による保管

DEHP の捕集後，プレートは GC/MS による分析まで保管する必要がある。そこで，DEHP を捕集したプレートを SUS 保管容器内に保管した後，プレートに残っている DEHP 量を測定し，保管における DEHP の減少量を把握した。この容器はプレート端部を挟み込み，容器とプレート表面部が直接接触することなく保管できる容器である。試験方法は，1.2 で検討した方法を用いて，石英プレートに DEHP を吸着させた後，プレートを保管容器に入れ，25℃，40%の恒温槽で 1 日および 3 日間保管した。マイクロチャンバは試験後，すぐに加熱脱着を行なってチャンバに吸着した DEHP の測定を行なった。その後，プレート単体に吸着した DEHP 量を測定した。この時の測定条件は，1.2 と同一である。

1.6　サンド容器による保管

保管時における DEHP の低減を防ぐために DEHP 捕集した石英プレートの上面と下面に同一素材のプレートで挟み込んで，再放散する DEHP をプレートで捕捉することにより DEHP の低減を防ぐ方法を検討した。この方法を便宜上サンド保管と呼ぶ。サンド保管の概要を図 - 8 に示す。

図 - 8　サンド保管の概要

試験方法は，1.2で検討した配置方法でプレートにDEHPを捕集した後，捕集プレートの上面および下面に同一のプレートで挟み込み，その上からアルミ箔で包んで，25℃.40%で1日および3日保管した。その後，マイクロチャンバで捕集プレートおよびサンドに用いたプレート2枚に吸着したDEHP量を測定した。測定条件は1.2と同一である。

2. 結　果

2.1　プレート素材の検討（材料のSVOCs放散量測定）

フロアーマットから放散した成分の測定結果を図9に示す。縦軸には，発生ガスとして気中に拡散した量をAirとして，チャンバ壁面に吸着した量をchamberとして標記した。この結果よりDEHPは壁面に吸着していることがわかった。一方，C14などの成分はそのほとんどが気中に存在していることがわかった。そして，今回用いた部品からは目的成分であるDEHPが平均値として3025ng検出できた。また，この時のCV値は約8%と良好な結果であった。

次に，約1年間の継続測定の平均値は2900ng（n=10）であり，初期計測値である3025ngと比較して誤差4%であり，継続したDEHPの放散が見込める材料であることがわかった。

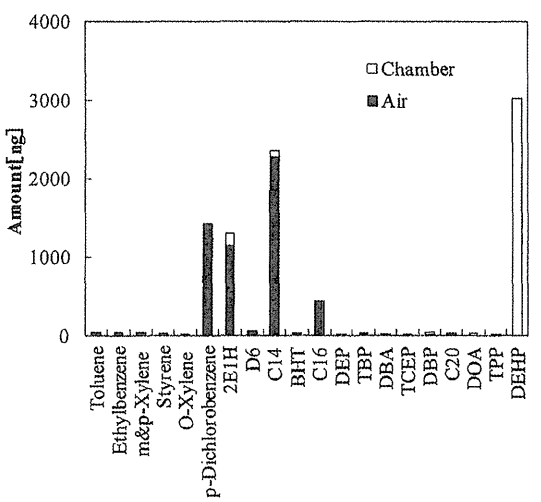

図-9　フロアーマットからのDEHP量測定結果平均値（n=9）

2.2　部品とプレートの配置の検討

フロアーマットとプレート配置の違いにおけるDEHP放散量の測定結果を図-10に示す。この結果より，部品をプレートの上に配置した方が，DEHPの捕捉量が多くなることがわかった。また，部品とプレートの間隔を5mmと10mmで比較したが，10mmの方が1.7倍と捕捉効率が良かった。また，プレートに部品が直接接触する場合は，捕捉効率が悪くCASE2-2の20%程度であった。この理由はプレートそのものが部品からの拡散を妨げているようになるため捕捉効率が低下したと推測される。

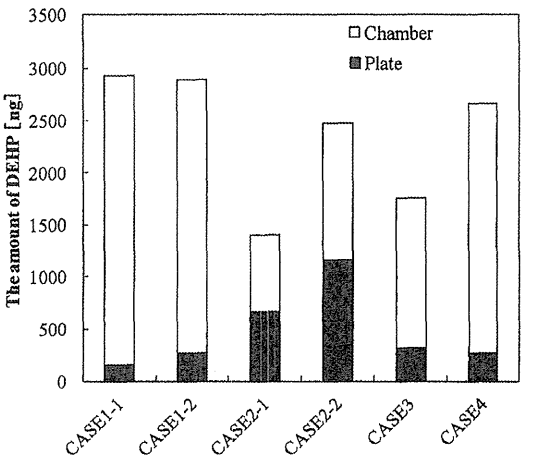

図-10　試料およびプレート配置とDEHP捕集量の関係（n=3）

2.3　数値解析によるプレートへのDEHP捕捉効率の検討

マイクロチャンバ内に設置した部品から揮発したDEHP濃度の数値計算結果を図-11，12，表-6に示す。X軸断面およびY軸断面の結果は同一であったため，Y軸断面の結果のみを示す。この結果より，チャンバ内の材料からDEHPが下方に設定したプレート上面方向にダウンフローの形成が確認でき，材料から放散したDEHPがプレート面に流れ込んでいることがわかる。また，濃度分布結果より材料下面におけるDEHP濃度が高い傾向であることがわかった。また，DEHP吸着量結果の比較より，チャンバおよびプレートの表面積比が2.5：1に対して，実験値は1.3：1であった。一方、数値解析結果では、1.7：1であった。数値解析の結果から，プレート上面にDEHPの殆どが吸着していると推測されることから，実際の面積比率は5：1になると推測される。このことから，表面積比とプレートへのDEHP吸着量比は乖離しているが，実験値と数値解析値が比較的近い値であることから，チャンバへのDEHP吸着量が低下したのではなく，プレートへのDEHP吸着量効率が良かったために面積比率とDEHP吸着量は乖離したと推測される。今回の数値解析条件は，チャンバ壁面に吸着ありとして解析を実施したため，チャンバ外への排出量は無視できる程度であった。また，プレート上面へのDEHP吸着が殆どであった。